

Conf-910435--86

UCRL-JC-104754  
PREPRINT

Received by

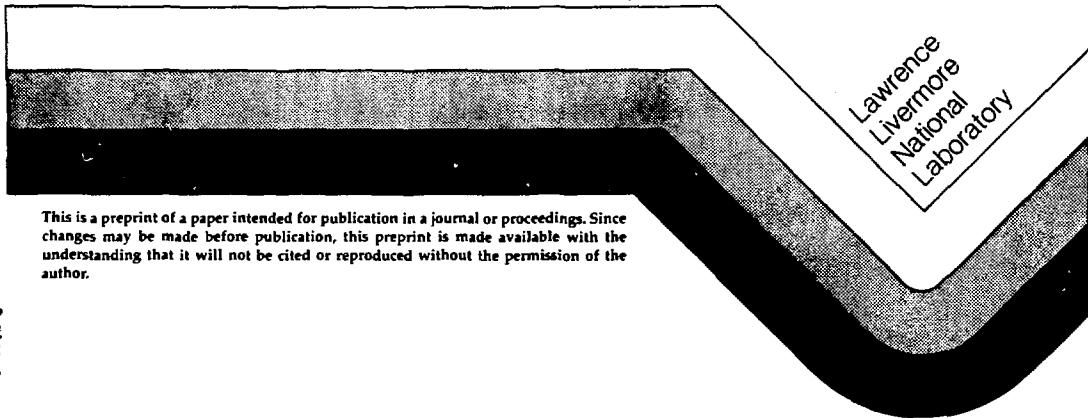
JUN 10 1991

EFFECTS OF HETEROGENEITY ON ACTINIDE  
DIFFUSION RATES IN TUFFACEOUS ROCK

Marilyn Buchholtz ten Brink  
Douglas L. Phinney  
David K. Smith

This paper was prepared for submittal to  
International High Level Radioactive Waste  
Management Conference, Las Vegas, NV  
April 28 - May 2, 1991.

Manuscript Date: December 1990  
Publication Date: April 1991



This is a preprint of a paper intended for publication in a journal or proceedings. Since changes may be made before publication, this preprint is made available with the understanding that it will not be cited or reproduced without the permission of the author.

MASTER

DISTRIBUTION OF THIS DOCUMENT IS UNLIMITED

## DISCLAIMER

This document was prepared as an account of work sponsored by an agency of the United States Government. Neither the United States Government nor the University of California nor any of their employees, makes any warranty, express or implied, or assumes any legal liability or responsibility for the accuracy, completeness, or usefulness of any information, apparatus, product, or process disclosed, or represents that its use would not infringe privately owned rights. Reference herein to any specific commercial products, process, or service by trade name, trademark, manufacturer, or otherwise, does not necessarily constitute or imply its endorsement, recommendation, or favoring by the United States Government or the University of California. The views and opinions of authors expressed herein do not necessarily state or reflect those of the United States Government or the University of California, and shall not be used for advertising or product endorsement purposes.

## EFFECTS OF HETEROGENEITY ON ACTINIDE DIFFUSION RATES IN TUFFACEOUS ROCK

Marilyn Buchholtz ten Brink<sup>a</sup>, Douglas L. Phinney<sup>b</sup>, David K. Smith<sup>a</sup>  
 Earth Science Department<sup>a</sup> and Nuclear Chemistry Division<sup>b</sup>  
 Lawrence Livermore National Laboratory  
 L-202 P.O. Box 808  
 Livermore, California, 94550  
 415-423-7662

## ABSTRACT

The pore structure and mineralogy of Topopah Spring Tuff are heterogeneous on scales less than one cm. This heterogeneity creates spatial variation in transport rates for aqueous actinide species both on the scale of tenths of microns and the scale of mm. The volumetric distribution of fluid paths having very different tortuosity, and potentially differing surface mineralogy and sorptive properties, must be considered in order to provide realistic predictions of transport rates. In addition, size and speciation of actinides in solution must be characterized since coexisting species can diffuse at different rates through the porous material due to both filtration effects and differences in sorption onto exposed mineral surfaces.

## I. INTRODUCTION

Diffusive transport rates for aqueous species in porous media are a function of the molecular diffusion rate in solution for the species of interest, any change in its concentration in solution due to sorption or reaction, and the tortuosity of the material's pore structure. Diffusion rates can be easily predicted when these factors are known and constant; however, this is not the case for heterogeneous natural materials, such as Topopah Spring Tuff, and the complex solutions derived from many hazardous wastes.

Coexistence of multiple oxidation states, colloidal species, and numerous complexes for actinide elements in ground or waste-water solutions suggests that a range also exists for molecular diffusivity, reactivity, and sorptivity. The physical structure of a rock includes void spaces on scales from grain boundaries and intergranular pore spaces to fractures that are centimeters in width. The chemical structures of rocks such as tuff are also heterogeneous; void spaces may be filled with secondary phases and fractures lined with precipitates, while phenocrysts and inclusions abound throughout the rock. Diffusive movement of aqueous species within the rock then depends on the effective length of the voids and their interconnectedness, i.e. the tortuosity of any diffusive path. The sorptive capacity of each mineral

phase for the aqueous species of interest can differ by orders of magnitude. Differing sorptive mechanisms can also result in large differences among minerals for reversibility and kinetics of sorption.

This complicated heterogeneous system makes a mechanistic prediction of diffusion rates difficult without information about the relative importance of the different factors. An understanding of the effect of multiple transport paths and sorption mechanisms is particularly important for planning containment of hazardous materials since a small amount of radioisotope travelling via a faster than anticipated path (Table 1) may invalidate the predictions of transport models that assume homogeneous or average behavior. Consequently, the heterogeneity of actinide diffusion in Topopah Spring tuff was investigated in static-diffusion experiments in which aqueous <sup>238</sup>U, <sup>235</sup>U, or <sup>239</sup>Pu tracer diffused into tuff that was pre-saturated with groundwater.

Table 1. Near field geochemical and hydrological transport processes affected by chemical or physical heterogeneity

Transport Process	Radioisotope mobility	
	Enhanced	reduced
Fluid advection (fracture flow)	✓	
Fluid diffusion (matrix imbibition)		✓
Intermittent flow	✓	✓
Sorption		✓
Precipitation (onto mobile/immobile phases)	✓	✓
Colloid filtration		✓
Fracture sealing		✓
Channeling	✓	

## II. DESCRIPTION OF WORK

Experimental conditions were as follows: all experimental Radiotracers that had pre-equilibrated with groundwater from well J-13 (which contacts Topopah Spring tuff *in situ*) diffused into samples of Topopah Spring tuff rock, the proposed repository horizon material for high-level waste in the U.S.A.. The tuff

was obtained from drill core, machined to specified sizes, cleaned, and saturated to >70% by immersion in J-13 well-water prior to contact with radiotracers.

experiment 1) The radiotracers were  $^{238}\text{U}$  and  $^{239}\text{Pu}$  leached from actinide-containing borosilicate glass, the experiment was at 90°C in stainless steel (306L) containers and tracers diffused into 0.2 cm thick by 2.5 cm diameter tuff disks for 14 d, 28 d, 56 d, 91 d, and 182 d. Further experimental details are given in Phinney et al.<sup>1</sup>

experiment 2) The radiotracer was 2 ppm  $^{238}\text{U}$  pre-equilibrated with J-13 water, the experiment was at 25°C in stainless steel (306L) containers and the tracer diffused into 0.2 cm thick by 2.5 cm diameter tuff disks for 1 min, 20 min, 2 hr, 8 hr, 4 d, and 14 d. Further experimental details are given in McKeegan et al.<sup>2,3</sup>.

experiment 3) The radiotracer was 2 ppm  $^{235}\text{U}$  pre-equilibrated with J-13 water and  $\text{NaHCO}_3$ , the experiment was at 25°C in polyethylene (HDPE) containers and the tracer diffused into 0.2 cm thick by 2.5 cm diameter tuff disks for 8 hr. Further experimental details are given in McKeegan et al.<sup>3</sup>

experiment 4) The radiotracers were 80 ppb  $^{238}\text{U}$  and 20ppb  $^{239}\text{Pu}$  leached from actinide-containing borosilicate glass, the experiment was at 90°C and the tracers diffused from the interior to exterior of a tuff vessel with 2 cm thick walls for 183 days. Tuff was obtained from Fran Ridge outcrop. Further experimental details are given in Bazzin et al.<sup>4</sup>

$\text{PuO}^+$  and  $\text{UO}^+$  concentrations were measured in the tuff with a CAMECA IMS-3f secondary ion mass spectrometer (SIMS) equipped with a resistive anode encoder (RAE) detector (Figure 1). The distributions of  $\text{Li}^+$ ,  $\text{Al}^{++}$ ,  $\text{Si}^{++}$ ,  $\text{Zr}^+$  and  $\text{B}^+$  were measured in conjunction with the actinides while major elements were also determined in some cases. Areas (60  $\mu\text{m}$  in diameter) in the fine-grained matrix<sup>5</sup> were selected for analysis at random on the surface of the tuff that had been exposed to radiotracers. Concentration vs. depth was measured parallel to the transport path every 0.1  $\mu\text{m}$  in the upper 20  $\mu\text{m}$  (depth-profiling mode). Spatially oriented concentrations within the analysis spot were obtained for samples from experiments 2 and 3 with the RAE (imaging mode). Concentrations in the interior of some of tuff samples from experiments 3 and 4 were measured both perpendicular and parallel to the transport path every 50  $\mu\text{m}$  (step-scan mode). Corrections were made for surface roughness and sample drying effects<sup>3</sup>. Apparent diffusion coefficients ( $D_{\text{app}}$ ) were calculated from profiles of tracer-concentration vs. depth of <20  $\mu\text{m}$ ,<sup>3</sup> where the concentration was the total observed in the analysis spot.  $D_{\text{app}}$  values were also calculated from concentrations measured in the interior of the tuff (1.01-2 mm depth)<sup>6,7</sup>.

*Secondary (SEM) and back-scattered (BSE) electron imaging of the tuff samples allowed examination of large areas on the samples and helped identify mineralogy, pore structure, and the presence of micro-fractures. The size distribution of porosity in the tuff samples was determined with image processing and mercury porosimetry. The chemical composition of the actinide-groundwater solution was determined with ICP-ES, ICP-MS, ion chromatography, and liquid-scintillation detection. The particle-size distribution of actinide complexes in solution was determined for some of the solutions by ultra-filtration and auto-correlated photon spectroscopy.*

## III. RESULTS AND DISCUSSION

Apparent diffusion rates for U or Pu in Topopah Spring tuff matrix vary by 80% on the average between locations (3.6  $\text{mm}^2$  area) measured on the same sample (Table 2). Regions of greater actinide concentration are associated with either greater porosity, identifiable micro-fractures, or concentrations of specific elements (Figure 2). Even greater spatial variability in concentration-depth profiles is observed with images obtained using the RAE detector which allows spatial resolution on a scale of a few microns.

### A. Physical heterogeneity

Uranium concentrations were elevated above background levels in the interior of the tuff samples, well beyond depths expected from assumptions of transport by a single diffusion coefficient in a homogeneous porous medium<sup>6,7</sup>. The distribution of interconnected pores in the tuff is approximately 95% of the pore volume in

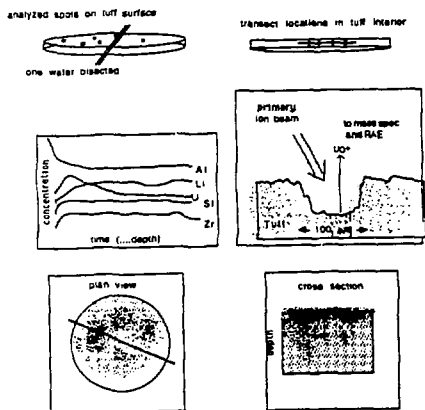


Figure 1. Schematic of analysis location and data generated with secondary ion mass spectrometry.

## Diffusion of Uranium solution in Topopah Spring Tuff

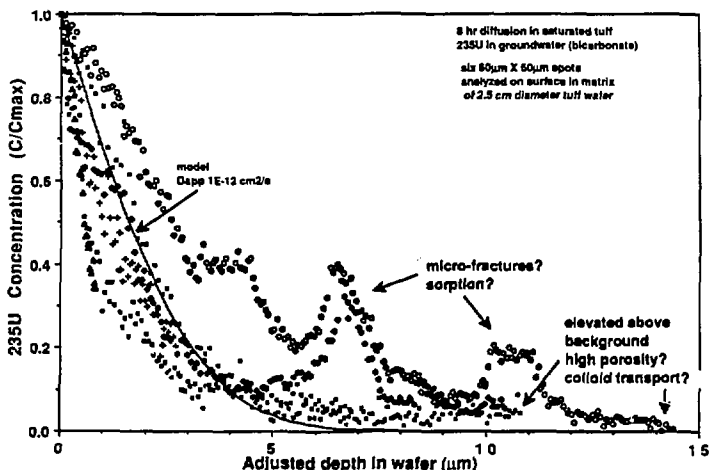


Figure 2. Uranium concentration vs. depth in tuff wafer showing evidence of physical and chemical heterogeneity on diffusive transport.

### Pore Size Distribution for Topopah Spring Tuff

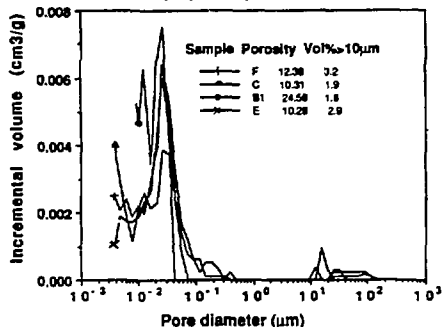


Figure 3. Distribution of pore-size in Topopah Spring tuff.

pores of .01 - 1 μm (mean .03 μm) while about 5% of the pore volume is in pores with 10-100 μm equivalent diameter (Figure 3). The regions of elevated U concentration in the interior were in regions identified as having more of the 10-100 μm pores or micro-fractures (Figure 4)<sup>7</sup>. Resistive anode encoder images (Figure 5) indicate that the spatial variability associated with enhanced transport in more porous regions also exists on scales of microns.

Assuming that the  $D_{app}$  measured in the interior of  $10^{-8}$  to  $10^{-9}$   $cm^2/s$ <sup>6,7</sup> is valid for the ~5% volume of larger pores (a fast path) allows correction of the surface concentration profiles to obtain a "matrix"  $D_{app}$  between  $10^{-12}$  and  $10^{-13}$   $cm^2/s$  for experiment 3. This dual-porosity model explains the shape of the tracer profiles (e.g. Figure 2) observed in all of the tuff diffusion experiments and the elevated U concentrations observed below ~7 μm in that these can be attributed to transport of aqueous U species through the macro-pores or micro-fractures. The typical steep slope near the surface and gradual slope deeper in the concentration-vs.-depth profile has been identified in other systems having dual porosity<sup>8</sup> while materials having uni-modal porosity do not show the tailing at depth.

The variability in tracer concentration measured at any given depth on a single tuff sample decreases as the time for diffusion increases. This is observed both for the 0.1 μm spatial resolution images obtained with the RAE and the apparent "matrix" diffusion coefficients ( $D_{app}$ ) calculated from tracer concentrations integrated over 3.6  $mm^2$  area (Table 2). The ratio of small pores (matrix) to large pores (micro-structure) in the analyzed region that are exposed to radiotracer solution increases with time for diffusion (Figure 6). Hence, the inappropriate interpretation of the combined "matrix" slow path and "fracture" fast path as equivalent routes for diffusion in a homogeneous media results in an apparent time dependency of the bulk diffusion coefficient<sup>2</sup>.

**Table 2.**  
**DIFFUSION PARAMETERS (a) FOR ACTINIDES IN TUFF**

EXP <sup>(b)</sup>	SAMPLE	TIME	SPOT #	ISOTOPE	D <sub>app</sub> cm <sup>2</sup> /s (c)	Average D <sub>app</sub> cm <sup>2</sup> /s (±1σdev)
1	G-231	14 d	1	<sup>239</sup> Pu	2.003E-16	4.20E-16
			2		4.532E-16	±1.37E-16
			3		5.318E-16	33%
			4		3.894E-16	
1	G-233	28 d	1	<sup>239</sup> Pu	3.879E-16	3.18E-16
			2		1.817E-16	±2.23E-16
			3		1.036E-16	70%
			4		6.007E-16	
1	G-235	56 d	1	<sup>239</sup> Pu	7.244E-17	2.04E-16
			2		3.119E-16	1.48E-16
			3		8.111E-17	73%
			4		1.501E-16	
			5		4.067E-16	
1	G-237	91 d	1	<sup>239</sup> Pu	1.407E-16	2.29E-16
			2		1.598E-16	±1.41E-16
			3		1.747E-16	62%
			4		4.398E-16	
1	G-239	182 d	1	<sup>239</sup> Pu	7.174E-17	6.50E-17
			2		7.744E-17	±3.11E-17
			4		4.078E-17	48%
			5		1.068E-16	
			9		2.843E-17	
2	wafer 6	1 m	1	<sup>238</sup> U	1.77E-10	9.71E-11
			2		2.99E-11	±7.44E-11
			3		8.436E-11	77%
2	wafer 1	20 m	1	<sup>238</sup> U	1.089E-12	2.71E-12
			2		1.086E-12	±4.05E-12
			3		5.017E-13	150%
			4		9.26E-13	
			5		9.943E-12	
2	wafer 2	2 hrs	1	<sup>238</sup> U	1.261E-13	2.86E-13
			2		3.983E-14	±3.87E-13
			3		9.64E-13	135%
			4		5.796E-14	
			5		2.443E-13	
2	wafer 3	8 hrs	1	<sup>238</sup> U	1.285E-13	5.15E-14
			2		7.844E-14	±5.12E-14
			3		2.852E-14	100%
			4		1.499E-14	
			5		6.864E-15	

EXP <sup>(b)</sup>	SAMPLE	TIME	SPOT #	ISOTOPE	D <sub>app</sub> cm <sup>2</sup> /s (c)	Average D <sub>app</sub> cm <sup>2</sup> /s (±1σdev)
2	wafer 4	4 d	1	<sup>238</sup> U	6.448E-15	1.60E-14
			2		5.628E-14	±1.93E-14
			3		7.634E-15	121%
			4		4.203E-15	
			5		2.598E-14	
			6		6.198E-15	
			7		5.32E-15	
2	wafer 5	14 d	1	<sup>238</sup> U	3.492E-16	9.91E-16
			2		1.088E-15	±6.65E-16
			3		5.194E-16	67%
			4		1.442E-15	
			5		4.95E-15	
3	.05μm	8 hr	2	<sup>235</sup> U	1.731E-13	1.37E-12
			3		4.677E-13	±2.15E-12
			4		1.014E-12	158%
			5		2.997E-13	
			6		1.427E-13	
			7		5.707E-12	
			8		9.038E-13	
			3		.3μm	8 hr
2	1.464E-13	±8.86E-13				
3	3.679E-13	86%				
5	1.013E-12					
6	1.154E-12					
7	8.535E-13					
3	400 grit	8 hr		1		
			2	4.576E-12	±2.28E-12	
3	600 grit	8 hr	1	<sup>235</sup> U	7.26E-13	9.54E-13
			2		9.841E-13	±2.14E-13
			3		1.152E-12	23%
4	V9	183d	1	<sup>239</sup> Pu, <sup>238</sup> U	≤2E-16, ≤3E-15	

(a) Determined from SIMS concentration vs. depth profiles in the upper 15 μm  
 (b) Conditions for experiments 1,2,3,4 are discussed in the text  
 (c) This value is calculated for regions that appear to be matrix under low power magnification. Phenocrysts, fractures, and obvious subsurface peaks have been excluded for calculation

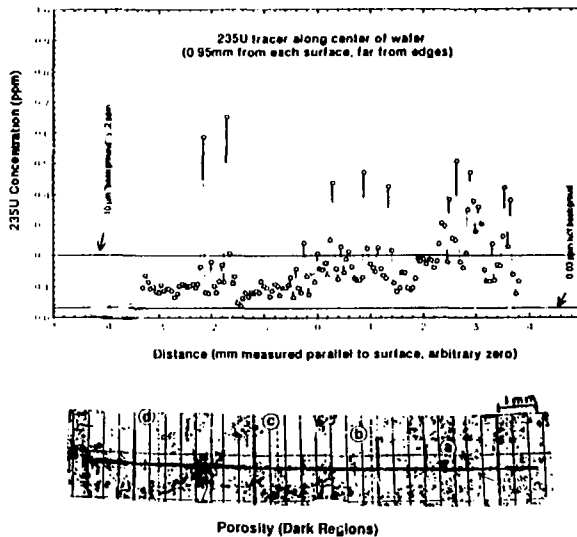


Figure 4. (a) Elevated Uranium concentrations in the interior of a tuff disk associated with (b) regions of greater porosity. The dark center line in (b) is the track of analysis shown in (a) and other dark regions are pores larger than 10  $\mu\text{m}$  in diameter.

## Fracture transport of U

8 hr (water 3) spot 2

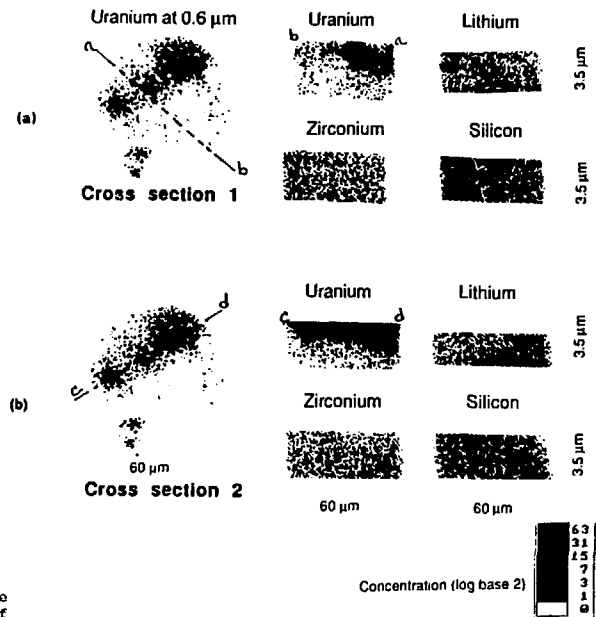
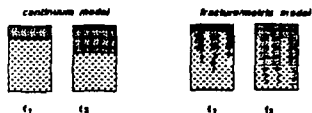


Figure 5. Elevated U concentrations associated with macroporosity or a micro-fracture.

In saturated diffusive systems:  
 95% of actinide transport occurs in the matrix (slow)  
 .5% occurs in microfractures (up to 1000 x faster)



In saturated advective systems:  
 most transport will occur in microfractures at the faster rate

In unsaturated systems:  
 transport will occur in microfractures (fast) only during high-flow rates  
 transport will generally occur in matrix (slow) and capillary films

Figure 6. Schematic effect of fracture-matrix model vs. continuum model on transport and observed concentration vs. depth profiles.

#### B. Chemical heterogeneity

Topopah Spring tuff has heterogeneous mineralogy on all of the scales over which actinide diffusion rates were measured, cm to .01  $\mu\text{m}$  <sup>5,3</sup>. Major-element mineralogy varies even within a 60  $\mu\text{m}$  diameter analysis spot (Figures 3 and 7) and affects the concentration of the tracer that sorbs to the solid phase<sup>3</sup>. Distribution coefficients for actinides on different pure minerals<sup>9</sup> can vary by as much as three orders of magnitude. Consequently, any tracer concentration measured for an analysis spot may actually be attributed to transport or retardation in just a small region of that area and Dapp values may not represent the true maximum or average value of the rock.

The chemical composition of the fluid also determines the rate of diffusive transport in the system in that sorption, precipitation and filtration are affected by the actinide speciation and size. Addition of sodium bicarbonate to U-groundwater solutions increased the apparent bulk diffusion coefficient by one to two orders of magnitude (Figure 8) and increased the abundance of colloidal-sized particles. Changes in speciation of the actinides in solution, e.g., formation of U-carbonate complexes, likely resulted in decreases in the amount of U retarded by sorption that are reflected in the faster transport rate for experiment 3 than experiment 2. Colloidal particles that approach the size of the average pores occur naturally in J-13 water<sup>10</sup> and are present in actinide-glass leach solutions<sup>11</sup>. The slower rate of "fracture" transport,  $D_{app} \sim 10^{-11}$  cm<sup>2</sup>/s, identified in the tuff interior for experiment 4 than for experiment 3 may also be attributed to association of the tracers with colloidal particles spalled off or formed from the actinide-glass<sup>7</sup>. Despite having zero charge

2 hour (water 2) spot 3 at 5.5  $\mu\text{m}$

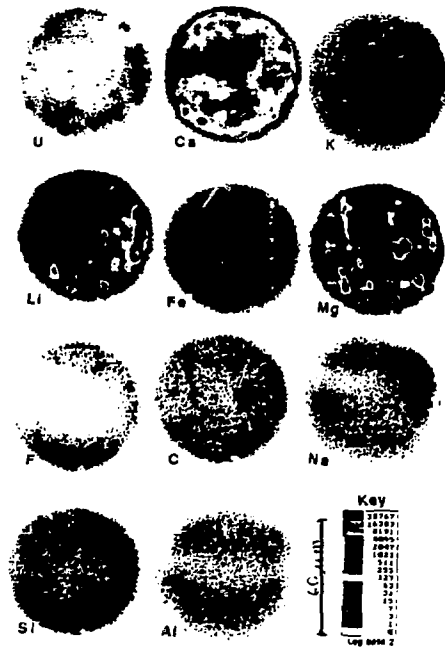


Figure 7. Elevated U concentrations associated with concentrations of other elements

and low tendency to sorb to the tuff minerals, transport for these particles may be retarded by filtration effects. Neither temperature (25°C - 90°C) nor dissolved tracer concentration appeared to have a discernable influence on the measured transport of aqueous actinide species in tuff.

#### IV. SUMMARY

The pore structure and mineralogy of Topopah Spring Tuff are heterogeneous on scales less than one cm. This heterogeneity creates spatial variation in transport rates for aqueous actinide species both on the scale of tenths of microns and the scale of mm. The volumetric distribution of fluid paths having very different tortuosity, and potentially differing surface mineralogy and sorptive properties, must be considered in order to provide realistic predictions of transport rates for hazardous materials in this type of geological material. In addition, actual size and speciation of actinides in solution must be identified since coexisting actinide species can diffuse at different rates through the porous material due to both size-filtration effects and



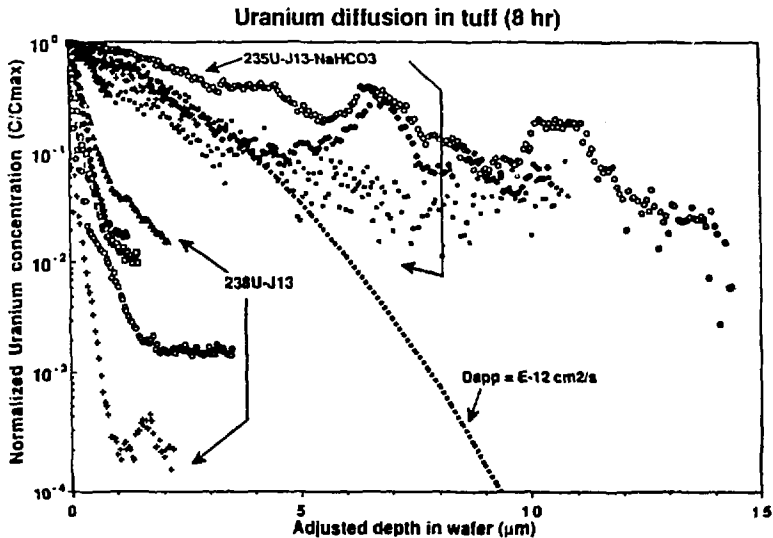


Figure 8. Comparison of U concentration vs. depth profiles in experiments having differing water chemistries.

differences in tendencies to sorb onto mineral surfaces exposed within the porous structure of the rock. It is clear that further measurements of radionuclide transport rates in coupled chemical-hydrological experiments are necessary to bound, validate and guide mechanistic models of transport processes for actinides in heterogeneous systems.

#### ACKNOWLEDGEMENTS

We thank Virginia Oversby, Kevin McKeegan, and James Wong for previous contributions to these experiments. Prepared by Yucca Mountain Site Characterization Project (YMSCP) participants as part of the Civilian Radioactive Waste Management Program. The Yucca Mountain Site Characterization Project is managed by the Yucca Mountain Site Characterization Project Office of the U.S. Dept. of Energy, Las Vegas, Nevada. Work performed under the auspices of the U.S. Dept. of Energy by Lawrence Livermore National Laboratory under contract No. W-7405-ENG-48.

#### REFERENCES

- <sup>1</sup>PHINNEY, D.L., F.J. RYERSON, V.M. OVERSBY, W.A. LANFORD, R.D. AINES, AND J.K. BATES, "Integrated testing of the SRU-165 glass waste form," UCRL 94658. pp 433-446 In: *Materials Research Society Symposia Proceedings: Scientific Basis for Nuclear Waste Management X*, Ed. J. Bates (1986)
- <sup>2</sup>K. MCKEEGAN, M.R. BUCHHOLTZ-TEN BRINK, V.M. OVERSBY, AND D.L. PHINNEY, "Ion-microscope observations of uranium transport in Topopah Spring Tuff" *EOS*, 68(44), 1282. (1987)
- <sup>3</sup>K. MCKEEGAN, D. PHINNEY, V.M. OVERSBY, M. BUCHHOLTZ-TEN BRINK, AND D.K. SMITH, "Uranium transport in Topopah Spring tuff: An ion-microscope investigation," UCRL 99734, In: *Materials Research Society Symposia Proceedings: Scientific Basis for Nuclear Waste Management XII*, 127, 813-821 (1988)

<sup>4</sup>F. BAZAN, J. REGO, AND R.D. AINES. "Leaching of actinide-doped nuclear-waste glass in a tuff-dominated system," UCRL 53745. pp447-458 In: *Materials Research Society Symposia Proceedings: Scientific Basis for Nuclear Waste Management X*. Ed. J. Bates, (1986)

<sup>5</sup>F.M. BEYERS AND L.M. MOORE. *Los Alamos National Laboratory Report No. La-10901-H5*, Los Alamos, New Mexico, 72 pp. (1987)

<sup>6</sup>M.R. BUCHHOLTZ TEN BRINK, D. PHINNEY, K.D. MCKEEGAN AND V.M. OVERSBY. "Uranium transport in Topopah Spring Tuff: multiple diffusion paths," Presented at "Chemistry and Migration Behavior of Actinides and Fission Products in the Geosphere", Nov 6-10, 1989, Monterey, Calif. (1989)

<sup>7</sup>M.R. BUCHHOLTZ TEN BRINK, D. PHINNEY, AND D.K. SMITH, "Actinide transport in Topopah Spring tuff: Pore size, particle size, and diffusion," In: *Materials Research Society Symposia Proceedings: Scientific Basis for Nuclear Waste Management XIV.*, Ed. J. Abrajano and L.H. Johnson, (1990) In press.

<sup>8</sup>K. IDEMITSU, H. FURUYA, R. TSUTSUMI, S. YONEZAWA, Y. INAGAKI AND S. SATO. "Migration of cesium, strontium and cobalt in water-saturated concretes," In: *Materials Research Society Symposia Proceedings: Scientific Basis for Nuclear Waste Management XIV.*, Ed. J. Abrajano and L.H. Johnson (1990) In press.

<sup>9</sup>K.V. TICKNOR, D.C. KAMINENI AND T.T. VANDERGRAAF, "Flow path mineralogy: Its effect on radionuclide migration in the geosphere," In: *Materials Research Society Symposia Proceedings: Scientific Basis for Nuclear Waste Management XIV.*, Ed. J. Abrajano and L.H. Johnson (1990) In press.

<sup>10</sup>M.R. BUCHHOLTZ TEN BRINK, S. MARTIN, B. VIANI, D.K. SMITH AND D.L. PHINNEY. "Heterogeneities in radionuclide transport: pore size, particle size, and sorption.," *Proceedings of Concepts in manipulation of groundwater colloids for environmental restoration.*, Manteo, N.C. Oct., 1990. In press. (1990)

<sup>11</sup>J.K. BATES, W.L. EBERT AND T.J. GERDING. "Vapor hydration and subsequent leaching of transuranic-containing SRL and WV glasses." In: *High Level Radioactive Waste Management Proceedings*, Vol.2 pp1095-1102, Publ Am. Nucl. Soc., LaGrange Park, Ill. (1990).